Generation of double-exponential EMC pulses with Software-Defined Radios

Marcelo B. Perotoni[1], Marcos S. Vieira[2], and Kenedy M. Santos[3]
[1]UFABC, Santo Andre, 09210-580, SP, Brazil
[2]Mackenzie Presbyterian University, Sao Paulo, 01302-907, SP, Brazil
[3]IFBA, Vitoria da Conquista, 45078-300, BA, Brazil

Corresponding author: Marcelo B. Perotoni (e-mail: marcelo.perotoni@ufabc.edu.br)

ABSTRACT This article presents a system to generate transient signals for EMC testing purposes. It is based on a low-cost commercial Software-Defined Radio (SDR) whose output contains the desired transient signal modulated by a higher-frequency sinusoidal. An envelope detector board removes the carrier so that the slow-varying curve is amplified to be used in the test setup. Due to the SDR nature, it is completely controlled by software, which enables a quick and easy operation able to synthesize different waveforms. An open-source software tool is used to control the SDR to generate the signal and set the carrier frequency. Here, the article focuses on double-exponential curves, very common in different EMC tests, but its application is not limited to them. A 5.9 μs risetime waveform is generated and tested against a real prototype representing a shielded cable over a ground plane. Individual building blocks are presented and the signal is analyzed as it goes through the cascade.

INDEX TERMS Electromagnetic Pulse, Software-Defined Radio, Pulse Measurement, Pulse generators

I. INTRODUCTION

PULSE generation is a very relevant function in conducted and radiated [1], [2], [3] immunity EMC tests and other types of electromagnetic evaluation. Controlled broadband current or voltage bursts help identify weak components inside a complex electronic system and are regulated by several different standards, depending on the field (e.g. automotive, aerospace, consumer electronics, etc). Pulses whose bands reach few MHz can be easily visualized with ordinary oscilloscopes [4] enabling a quick and affordable test setup. Within the waveforms suggested by the standards, a common analytical format used is based on the exponential.

The generation of transient signals for EMC testing purposes has been subject of active research. A conceptual block diagram for an UWB (Ultra-Wide Band) pulse generator [5] to be applied in conducted immunity testing has its pulse formed after summing up several independent sinusoidal carriers, starting from the MHz range. Different circuits are employed to synthesize EMC-related waveforms [4], usually based on RLC networks [6], [7], or only RC [8]. Designs based on passive components enable the generation of high-amplitude voltage or current levels. For the sake of component design, in [9] a Matlab code synthesizes arbitrary double-exponential curves based on RLC networks. In the case of high-voltage testing, [10] contains a list of different topologies and design rules. Double exponential waveform synthesis involves switching resistor and capacitors networks with the desired timing for the charge and discharge. Curve parameters are, however, defined by the individual components and their time constants. In case the devices are made to operate with high voltage or current levels their dimensions become large, so the system is no longer versatile, able to operate with different timing characteristics. Switching devices, in turn, can be thyristors, IGBTs, and even spark gaps for large-amplitude voltages and short switching times. In the case of HEMP (High-Intensity Electromagnetic Pulses) tests, high-amplitude, short electric fields are to be radiated in free space. To perform this task, one solution employed a TEM horn connected to a Marx Generator, an RC cascade sequentially switched by spark gaps, and it was able to produce pulses shorter than 10 ns [11].

One of the most common waveforms in EMC testing follows the analytical double-exponential equation, where V_o is the maximum amplitude, α and β are the decay and risetime constants, respectively.

$$v(t) = V_o \left[e^{-\alpha t} - e^{-\beta t} \right]. \tag{1}$$

its spectrum can be written as (ω stands for angular frequency) [12]:

$$V(\omega) = V_o \left[\frac{\beta - \alpha}{\alpha\beta + j\omega(\alpha + \beta) - \omega^2} \right]. \tag{2}$$

Table 1 contains some common EMC applications for this particular waveform along with their respective parameters. Fig. 1 contains the normalized generic curves in both time and frequency domains, also showing relevant timing markers used in the standards. Each curve characteristic is related to the α and β parameters, to be later used in the proposed application software. Timing definitions, however, involve

ambiguous parameters and concepts, so some common formats such as rise time and variants are supposed to be deprecated [13]. For instance, civilian aerospace standard DO160 definitions for risetime t_r and fall time t_f (sometimes called as duration) consider the first to be the interval it takes to reach the peak value (t_p) and the latter the duration between 50% values ($tf_{50\%} - tr_{50\%}$ as in Fig. 1). IEC standards, in turn, have their parameters defined in terms of front time $T1$ and tail time $T2$, described as [8], [10], [14]:

$$T1 = 1.67\,(t_{90\%} - t_{30\%})\,. \tag{3}$$

$$T2 = tf_{50\%}. \tag{4}$$

Since identifying the origin point may not be easy when using an oscilloscope, [14] also contains a rule to find it indirectly from the acquired 30% and 90% voltages ($t_{30\%}$ and $t_{90\%}$).

NEMP (Nuclear Electromagnetic Pulse) standards usually directly define both α and β parameters, with their risetime and fall times following the DO160 scheme. NEMP curves model the effects caused by electric fields radiated after nuclear explosions due to Compton Effect and gamma-ray emissions [15], and are a particular case of HEMPs, such as lightning, with the difference that they are of artificial nature. Three double-exponential curves are suggested in the open literature to model the effects right after the explosion: Early (E1), Intermediate (E2), and Late Time (E3), whose energies reach approximately 10 MHz [14]. In addition to these three curves, Bell Labs has also introduced its version of it, differing by its longer tail [16]. Duration time for the NEMP curves is also called Full-Width Half-Maximum (FWHM).

Electrostatic Discharge tests (ESD), used for conducted immunity, also employ pulses based on double exponentials [17], modeled after a sum of two signals, fast and slow [18]. Another immunity test application, Electrical Fast Transient (EFT) [19], usually contains several bursts applied by means of a capacitive coupling clamp. Their pulses are defined with rise and fall times similar to the DO160 standard. [20] reports the design of a 5 ns EFT pulse, with 75 bursts every 300 ms, based on a commercial FPGA core.

Standards also contain information on allowed variations around the nominal timing parameters, for instance [21] defines 10% for both $T1$ and $T2$ values whereas DO160 admits margins of 20% [22]. More details are found in each standard.

For this present study, α and β were set similar to the aerospace DO160 standard curve, with slightly shorter rise and fall-times. A low-level waveform is generated, adequate to be used in small-scale laboratory tests. Further scaling-up to the required voltage and current levels demanded by standards require other blocks. In addition to output level, its nature need to be taken into account - NEMP simulators employ large structures to radiate the broadband pulse as an electric field, whereas ESD and lightning pulses are usually of current type.

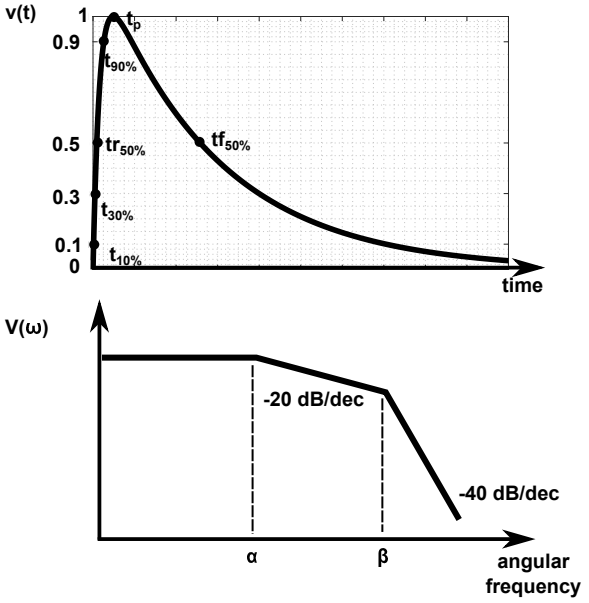

FIGURE 1. Generic double exponential waveform in time (top) and frequency (bottom) domains. It was considered normalized amplitudes for both cases.

TABLE 1. Parameters for some Double Exponential Functions in EMC - normalized amplitude.

Application	α [1/s]	β [1/s]	Rising time	Falling time
Lightning DO160 and MIL-STD-464 [22] [23]	11,354	647,265	t_r = 6.4 μs	t_f = 69 μs
NEMP E1 [14]	4E7	6E8	t_r = 4.88 ns	21.97 ns
NEMP E2 [14]	1E3	6E8	t_r = 0.24 μs	0.69 ms
NEMP Bell [16]	4E6	4.76E8	t_r = 0.01 μ	t_f = 0.17
Lightning Type 1 IEC 60060 [21]	14E3	25e5	$T1$ = 1.2 μs	$T2$ = 50 μs
Lightning Type 2 IEC 60060 [21]	5E4	17.3E4	$T1$ = 8	$T2$ = 20
EFT [19]	1.8E7	3.1E8	$t_{r10to90}$ = 5 ns	t_{f50} = 50 ns
ESD fast wave [17] [24]	8.3E10	5E10	$t_{r10to90}$ = 1.2 ns	t_{f50} = 2 ns
ESD slow wave [17] [24]	4.5E11	5E11	$t_{r10to90}$ = 22 ns	t_{f50} = 20 ns
This study	15,354	647,265	t_r = 5.90 μs	t_f = 51.7 μs

This paper presents the use of a commercial low-cost SDR to generate arbitrary time-domain waveforms. The versatility offered by the software- defined radio enables a quick and easy modification of the output signal, such as rise and fall times as well as pulse repetition frequency, for the case of tests requiring sequential bursts, e.g. the 14 to 20 [25] pulses used to emulate multiple strokes hitting a target. The com-

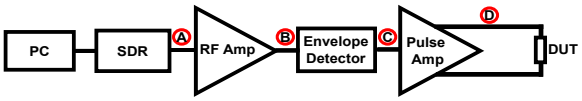

FIGURE 2. Block diagram of the system.

plete system can be expanded to reach higher amplitudes, in terms of currents, voltages, or electric fields. It can therefore be used as a building block in pre-compliance tests and even in EMC laboratory classes [7]. The next sections cover the building blocks, followed by the software and hardware components in more depth. A laboratory test is implemented, using a small-scale metallic tube electromagnetically coupled to an internal wire which is subject to the generated waveform, to visualize the complete system and its use.

II. SYSTEM BLOCK DIAGRAM

SDRs have become popular due to their lower costs and widespread information on their use in general applications. Low-cost alternatives are sometimes open-source, so they enable mass-produced units without the need for rights and royalties. Particularly regarding EMC applications, an SDR was used as the receiver in near-field measurement and compared with commercial systems for a PCB board test [26]. An NI USRP SDR, full-duplex and with 12 bits ADC, is compared to an Arbitrary Waveform Generator, regarding modulated signals in EMC [27], however, differing from the transient pulses here analyzed. The SDR here employed, Hack RF One, covers a bandwidth from 10 MHz to 6 GHz. It contains an 8-bit analog-to-digital converter (ADC) which can cover a maximum bandwidth of 20 MHz at once. It operates in half-duplex mode, with transmitting and receiving functions. Since double-exponential pulses employed in EMC testing contain large portions of their energy around DC and lower frequencies, direct synthesis of the time-domain pulse is not convenient since it is outside the SDR operating band. As alternative, a higher frequency carrier modulates the slow-varying pulse, so that the SDR operation and its safety limits are preserved. Further external analog processing recovers the envelope signal which is then amplified to be used in the test. Fig. 2 contains the block diagram of the proposed system. The SDR is connected to a low-level RF amplifier (50 MHz to 6 GHz, 20 dB Gain at 2 GHz), which provides a higher amplitude to the next stage, envelope detector, and also protects the SDR from short-circuits and undesired reflections.

Given the SDR wide frequency range, its overall characteristic in either receiving and transmitting modes are not flat. Maximum amplitude output was observed around 100 MHz, for the VHF range. In regard to the carrier signal choice, higher frequencies would demand a more complex envelope detector design whereas lower frequencies would have not only a smaller output level at the SDR but also might be below the RF amplifier band. Therefore, a 100 MHz carrier was chosen throughout the design. Moreover, depending on the transient pulse of choice, the 100 MHz carrier might be not sufficient, for instance in the case of EFT pulses that require risetimes around 5 ns. It should then have a carrier frequency ten times larger to comply with the current design, though still within the Hack RF One operational bandwidth.

Standards specify the waveforms to be applied on the DUTs as either current or voltages, besides the case of NEMP curves which are defined as electric fields at a certain distance from the radiator. Voltage outputs are defined as open-circuits whereas current modes operate ideally as short-circuits [28]. That reflects on the choice of the Pulse Amplifier block - it might be a voltage or current type, depending on the case, besides the case when it matches to an antenna, typically 50 Ω. The current amplifier, for applications such as lightning [15], should ideally come after a voltage-to-current converter. The final stage before the DUT has, therefore, to comply with the desired amplitudes, eventually requiring high-power switching devices. Here, the pulse amplifier is defined as a single emitter-source block, for the sake of simplicity.

III. SYSTEM DESCRIPTION - SOFTWARE

One of the most common application interfaces to SDRs is the open-source GNU Radio suite [29]. It is based on C++ for time-critical blocks and driver routines and uses Python as a wrapper and interface, delivering a final Python script that can be run independently of GNU Radio, using only its libraries. GNU Radio Companion, a part of the GNU Radio suite offers the possibility of flowgraph design based on blocks. Each GNU Radio block represents different signal processing and visualization tasks, besides the SDR interface, performed by the block named osmocom. Fig. 3 shows the program used to deliver the double-exponential curve to the SDR, with the two plots (time and frequency) that help visualize the generated signal. An analytical equation is described in terms of a Python expression, whose parameters (α and β) are set by the user and stored in variables. The equation delivers a vector type variable, which is transformed to stream data-type and is used as input to the osmocom sink responsible for the SDR communication. The osmocom block, operating as a transmitter with the frequency of 100 MHz, assumes the slow-varying double exponential curve as its input as the envelope multiplying the 100 MHz sinusoid. The analytical expression then modulates the 100-MHz carrier which is output to the SDR coaxial connector. The pulse is repeated every 500 μs, this parameter is defined with a GNU Radio variable and modifiable on-the-fly.

Though here it was used GNU Radio from a laptop, it can be run within Linux distributions in lean microprocessor modules such as Raspberry PI, so that the whole setup can be made portable and with even smaller costs.

IV. HARDWARE

Fig. 4 shows the schematics of the envelope detector and pulse (low-frequency) amplifier, which connects to the DUT (device under test). Letters in red circles follow the block diagram depicted in Fig. 2. A Schottky diode (conduction

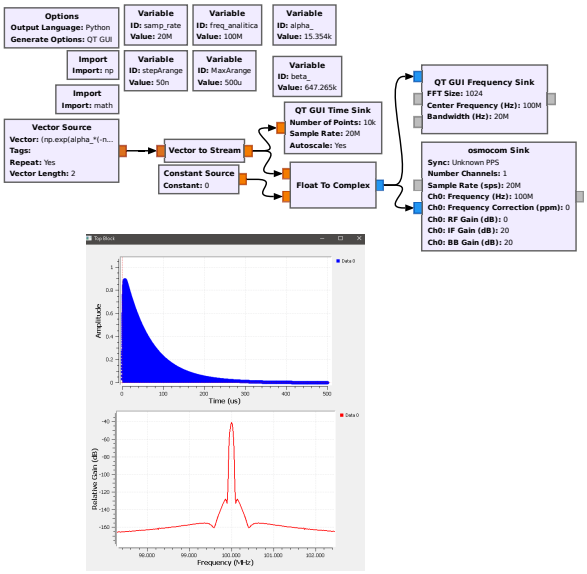

FIGURE 3. GNU Radio program and output plots (bottom).

voltage approximately 240 mV) operates as the core of an envelope detector, whose signal is then filtered by $R2$ and $C4$. The time-constant $\tau = R2 \cdot C4$ should lie between the frequencies of the modulated signal (i.e. the double exponential) and the RF carrier (100 MHz). $R1$ operates as both DC-path to the diode and proper load to the RF amplifier, while $C1$ is a DC-block. An external DC source $Vbias$ is applied to the diode, since the AC levels delivered from previous stages are not large enough to provide conduction of the diode. Final component values were chosen based on actual tuning, given the missing Schottky diode virtual model.

For the sake of a quick bench test, an ordinary Silicon BJT transistor 2N2222 (transition frequency f_T approximately 300 MHz and 1.5 W maximum power dissipation) is used as a common-emitter amplifier to deliver the pulse to a load. The DUT is inserted into the collector, to take advantage of the larger output swing. To the BJT was supplied a bias voltage of 12V.

Although the SDR has versatility in terms of rise times and other pulse characteristics adjusted on the fly, the envelope detector and subsequent hardware blocks need to operate within the spectrum content of the desired signals, particularly the envelope detector low-pass filter. Considering the usual pulse waveforms whose spectra reach tens of MHz, no special need is to be observed in the PCB layout or individual components, exception around the envelope detector. Chokes and decoupling capacitors were used in order to avoid RF contamination of the DC power supplies, as well as short leads and a large ground plane area.

V. WAVEFORMS ALONG THE CHAIN

The SDR output level is too small to overcome the conduction voltage of most signal diodes, so an RF amplifier is used. Fig. 5 shows the acquired waveforms, using a 200-MHz

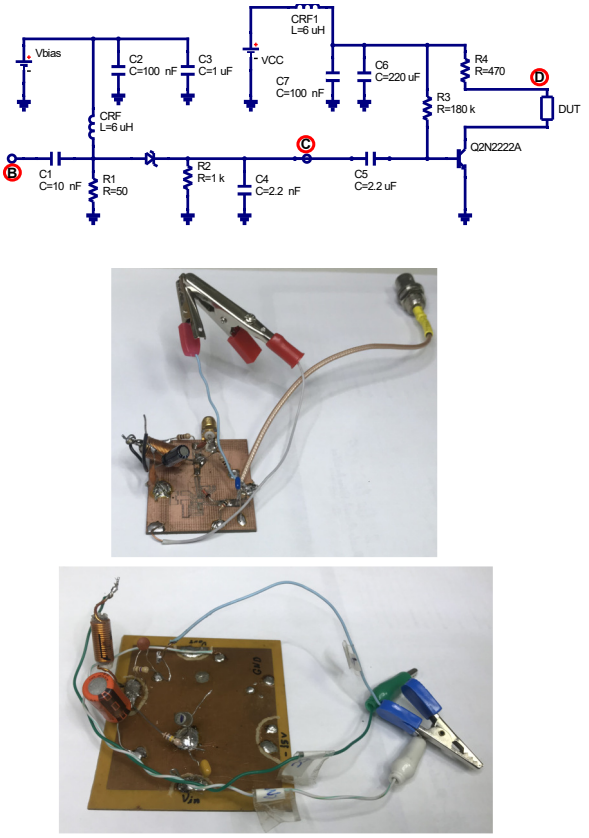

FIGURE 4. Schematic circuit (top) and respective envelope detector (center) and pulse amplifier (bottom) actual prototypes.

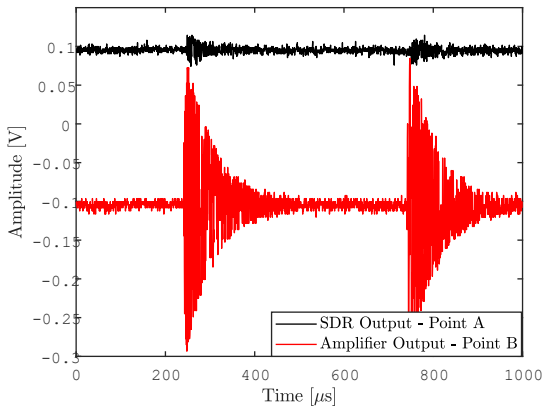

FIGURE 5. Output voltages taken at points A and B, respectively SDR and amplifier outputs. Note: Artificial DC offsets of ± 0.1V were added to ease the visualization of both curves.

oscilloscope with high-impedance probes, taken at points A and B as shown in Fig. 2, each case terminated in a 50 Ω load. It can be seen that right at the SDR output noise contaminates the pulse due to the low-level signal. Proper care has to be taken while choosing the right RF amplifier, another higher-gain unit (nominal gain of 62 dB up to 2 GHz) generated a distorted and noisy waveform.

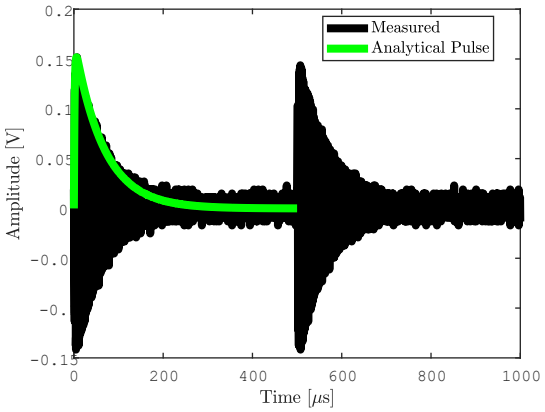

FIGURE 6. Comparison of the amplifier output and the analytical waveforms.

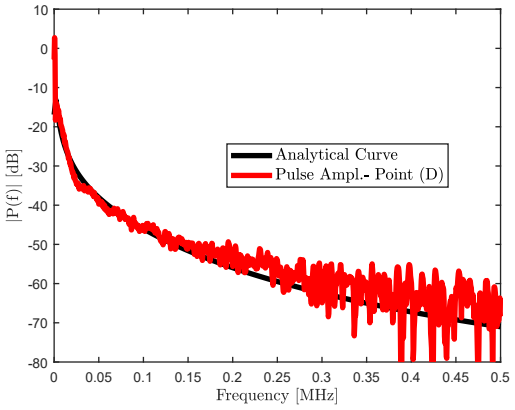

FIGURE 8. Power spectra comparison between the analytical pulse and measurement at point D, from Fig 2.

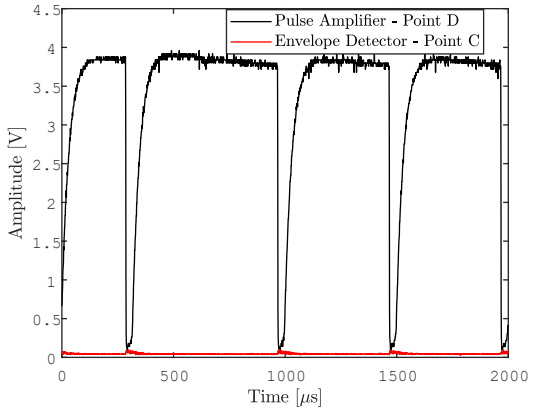

FIGURE 7. Measured signals at points C and D, from Fig 2.

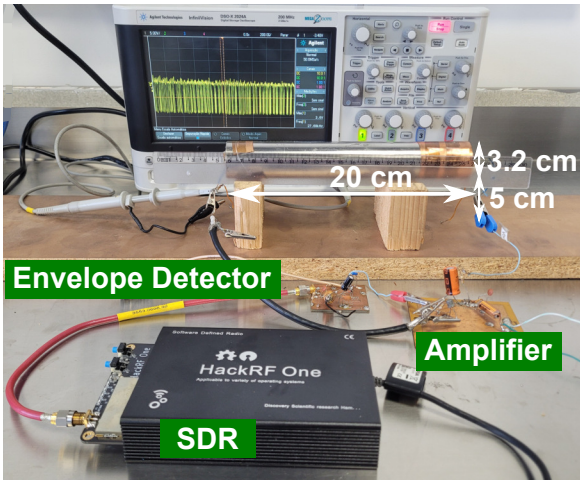

FIGURE 9. Complete test circuit, with the DUT dimensions.

For the sake of comparison, Fig. 6 contains the measured waveform in point B (after the RF amplifier) and the analytical expression, the latter normalized to its peak amplitude. It can be seen the good fidelity between both curves.

Finally, Fig. 7 contains pulses at either points C and D from Fig. 2, replacing the DUT component with a short-circuit. It can be seen that the transistor amplifier inverts the low-amplitude envelope detector pulse (common-emitter configuration) but also filters out the residual RF energy, due to its natural upper-frequency limit (around 4 MHz). V_{bias} was kept on 240 mV throughout the measurements.

Fig. 8 contains the normalized power spectra of both the analytical curve and the generated pulse at point D (pulse amplifier, short-circuited at the DUT terminals). It can be seen that both curves are similar, i.e. the joint frequency response of the cascaded block from the SDR output to the pulse amplifier does not introduce significant distortions in the desired double-exponential waveform. The result also shows that the generated signal contains energies much below the SDR frequency output range, given the employed modulation technique.

VI. REAL TEST

For the sake of a real application, the pulse is applied to a 1 mm diameter wire inside an Aluminum hollow tube (2mm thickness), as shown in Fig. 9. The geometry is based on the simulated case presented elsewhere [30], which investigated the shielding of a coaxial cable over a metallic ground plane. The pulses are applied to the wires, closing the final collector circuit in Fig. 4, point D in the schematic. Due to the coupling from the circulating current on the wire, voltages on the 20 kΩ resistors between the tube and ground plane are measured. The coupled signal is picked up by the oscilloscope over the resistors.

Fig. 10 plots the measured individual pulse at both resistors, shown inverted and with different time delays for ease the visualization, together with the analytical original pulse. It can be seen that only the high-frequency part of the incoming pulse is coupled.

By plotting the frequency spectra of both measured resistor voltages and the theoretical curve it is possible to see the high-pass characteristic of the coupling, (Fig. 11).

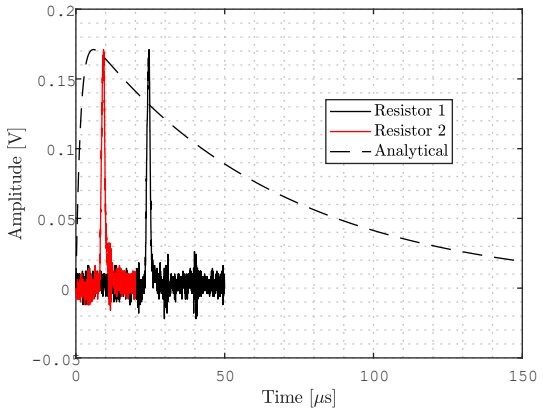

FIGURE 10. Measured induced voltages at both load resistors.

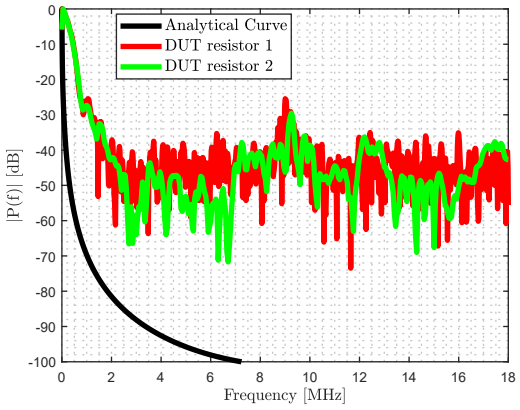

FIGURE 11. Spectra of the induced voltages at the load resistors and the analytical pulse. Results normalized to their maximum value.

VII. CONCLUSION

It is reported a method to generate arbitrary pulses to be used in transient EMC tests, based on a commercial SDR. A short survey of useful transient pulses, following double-exponential analytical curves, is also presented. They can be readily used by adjusting the timing parameters of the existing GNU Radio flowgraph. The system has low-cost (the HackRF One is currently sold under USD 400) and can be adjusted to outputs in current, voltage or electric field, depending on the chosen EMC standard, by means of the last stage amplifier. It offers advantages in terms of versatility, low cost and can be efficiently used in pre-compliance tests as well as experiments in EMC Laboratory courses. A test with the system was performed with the pulse applied to a wire inside a hollow metallic tube, in order to see the coupling on the external shield.

REFERENCES

[1] B. Ravelo, Y. Liu and A. K. Jastrzebski, PCB Near-Field Transient Emission Time-Domain Model., IEEE Trans. Electromagn. Compat., Vol. 57, No. 6, Dec. 2015, pp. 1320-1328.

[2] Y. Liu, B. Ravelo and A. K. Jastrzebski, Time-Domain Magnetic Dipole Model of PCB Near-Field Emission, IEEE Trans. Electromagn. Compat., Vol. 58, No. 5, Oct. 2016, pp. 1561-1569.

[3] B. Ravelo, Y. Liu, A. Louis and A. K. Jastrzebski, Study of high-frequency electromagnetic transients radiated by electric dipoles in near-field, IET Microw. Antennas Propag. (MAP), Vol. 5, No. 6, Apr. 2011, pp. 692-698.

[4] A. J. Schwab and W. Kürner, Elektromagnetische Verträglichkeit. Heidelberg, Germany: Springer, 2011.

[5] F. Brauer, R. Krzikalla, and J. L. ter Haseborg, "A concept for the generation of conducted ultra wideband pulses with high repetition rates," presented at the 2008 International Symposium on Electromagnetic Compatibility - EMC Europe, Hamburg, Germany, Sep. 8-12, 2008.

[6] G. Luo, W. Zhang, S. Huang, L. Qi, H. Wang, H. Ma, and J. Liu, "Equivalent circuit modeling of electro-magnetic pulse generator for typical immunity simulation," presented at the International Symposium on Electromagnetic Compatibility - EMC Europe, Angers, France, Sep. 4-8, 2017.

[7] F. Kugler, M. Albach, S. Schuh, and D.Kuebrich, "ESD laboratory for power electronics students," presented at the 2005 European Conference on Power Electronics and Applications, Dresden, Germany, Sep. 11-14, 2005.

[8] S. C. Dutta Roy and D. K. Bhargava, "On the design and generation of the double exponential function," IEEE Trans. Instrum. Meas., vol. 45, no. 1, pp. 309–312, Feb. 1986.

[9] P. Yutthagowith, and N. Pattanadech, "A Program for Design of Impulse Current Generator Circuits," presented at the International Conference on Condition Monitoring and Diagnosis, Beijing, China, Apr. 21-24, 2008.

[10] W. Hauschild W. and E. Lemke, High-Voltage Test and Measuring Techniques. Cham, Switzerland: Springer, 2019.

[11] M. R. Raju, V. V. R. Sarma, S. M. Satav, K. R. Rao, K. S. Narayana, and Z. H. Sholapurwala, "Fast Transient High Voltage Pulse Radiating System for vulnerability studies of NEMP on Electronic systems," presented at the 10th International Conference on Electromagnetic Interference & Compatibility, Bangalore, India, Nov. 26-27, 2008.

[12] P. Zydron, M. Kuniewski, and L. Fusnik, "Comparison of Pseudorandom White-noise Generators Used as Signal Source for Wideband Analysis of Transformer Windings Impedance," presented at the 9th International Scientific Symposium on Electrical Power Engineering (ELEKTROENERGETIKA), Stará Lesná, Slovak Republic, Sep. 12-14, 2017.

[13] IEEE Standard for Transitions, Pulses, and Related Waveforms, IEEE Instrumentation and Measurement Society, 2011.

[14] IEC 61000-2-9 Electromagnetic Compatibility (EMC) - Part 2: Environment - Section 9: Description of HEMP Environment - Radiated Disturbance, International Electrotechnical Commission, 1996.

[15] R. J. Perez, Handbook of Aerospace Electromagnetic Compatibility. Hoboken, NJ, USA: IEEE Press, 2009.

[16] R. K. Rajawat, R. S. Kalghatgi, and P. H. Ron, "A bounded wave transmission line type NEMP simulator-design, construction and field mapping," presented at the International Conference on Electromagnetic Interference and Compatibility, Hyderabad, India, Dec. 3-5, 1997.

[17] V. P. Kodali, Engineering Electromagnetic Compatibility: Principles, Measurements, Technologies. New York, NY, USA: IEEE Press, 1996.

[18] IEC 61000-4-10 Electromagnetic Compatibility (EMC) - Part 4-10: Testing and Measurement Techniques - Damped Oscillatory Magnetic Field Immunity Test, International Electrotechnical Commission, 2016.

[19] IEC 61000 Electromagnetic Compatibility (EMC) - Part 4-3 : Testing and Measurement Techniques - Radiated, Radio-Frequency, Electromagnetic Field Immunity Test, International Electrotechnical Commission, 2020.

[20] W. Zhu W., J. Zhang, Y. Zhang, and Yu J. and Wu S., "The Design of Signal Generator of Electrical Fast Transients Burst," Appl. Mech. Mater., vol. 336–338, no. 7, pp. 27–32, Jul. 2013.

[21] IEC 60060-1 High-Voltage Test Techniques - Part 1: General Definitions and Test Requirements, International Electrotechnical Commission, 2010.

[22] IEC 60060-1 RTCA DO 160 Environmental Conditions and Test Procedures for Airborne Equipment, Section 22, Lightning Induced Transient Susceptibility, Radio Technical Committee on Aeronautics, 2007.

[23] MIL STD-464C Electromagnetic Environmental Effects Requirements for Systems, US Department of Defense, 2010.

[24] R. K. Keenan, and L. A. Rosi, "Some fundamental aspects of ESD testing," presented at the IEEE 1991 International Symposium on Electromagnetic Compatibility, Cherry Hill, USA, Aug. 12-16, 1991.

[25] N. Wright, E. Sugrue, and M. Ermakov, "Recent developments in lightening test standards for aircraft and avionic," presented at the 6th International Symposium on Electromagnetic Compatibility and Electromagnetic Ecology, St. Petersburg, Russia, Jun. 21-24, 2005.

[26] R. T. Sánchez, M. S. Castañer, J. J. Foged, and D. Gray, "EMC Measurement System Based on Software Defined Radio and Diagnostic Techniques," presented at the Antenna Measurement Techniques Association Symposium (AMTA), San Diego, USA, Oct. 6-11, 2019.
[27] O. Kerfin, M. Schwar, and R. Geise R., "Arbitrary waveform generators anc software-defined radio for the synthesis of non-continuous wave EMC-test signals," presented at the International Symposium on Electromagnetic Compatibility - EMC Europe, Angers, France, Sep. 4-8, 2017.
[28] D. A. Weston, Electromagnetic Compatibility : Principles and Applications. New York, NY, USA: Marcel Dekker, 2001.
[29] GNU Radio Project. Available: https://www.gnuradio.org/, Accessed on: May 14, 2022
[30] Z. Ye, C. Liao, and C. Wen, "Time-Domain Coupling Analysis of Shielded Cable on the Ground Excited by Plane Wave," Prog. Electromagn. Res. M, vol. 67, pp. 45–53, 2018.